Inhalation of Nicotine-containing Electronic Cigarette Vapor Exacerbates the Features of COPD in βENaC-overexpressing Mice.

Xiangming Ji (xji4@gsu.edu)
Georgia State University https://orcid.org/0000-0002-5941-0253
Maureen Meister
GSU
Hongwei Han
GSU
Guangda Peng
GSU
Vu L. Ngo
GSU: Georgia State University
Odubade Oluwatosin
GSU: Georgia State University
Junqing An
GSU: Georgia State University
Jinjuan Qiao
GSU
Ping Song
GSU
Timothy Luke Denning
GSU
Jenny Yang
GSU
Ming-Hui Zou
GSU
Zhi-Ren Liu
GSU

Research

Keywords: Fibrosis, ENDS (Electronic Nicotine Delivery Systems), COPD (Chronic obstructive pulmonary disease)

Posted Date: December 16th, 2020

DOI: https://doi.org/10.21203/rs.3.rs-127494/v1

Inhalation of nicotine-containing electronic cigarette vapor exacerbates the features of COPD in βENaC-overexpressing mice

Authors

Maureen Meister[1*], Hongwei Han[2,3*], Guangda Peng[2], Vu L. Ngo[4], Odubade Oluwatosin[5], Junqing An[6], Jinjuan Qiao[5], Ping Song[6], Timothy Denning[4], Jenny Yang[5], Ming-Hui Zou[6], Zhi-Ren Liu[2], Xiangming Ji[1**]

Affiliation

[1]Department of Nutrition, Georgia State University, Atlanta, GA 30302; [2]Department of Biology, Georgia State University, Atlanta, GA 30303; [3]Division of Pulmonary and Critical Care, Department of Medicine, Massachusetts General Hospital, Boston, MA 02129; [4]Center for Inflammation, Immunity and Infection, Institute for Biomedical Sciences, Georgia State University, Atlanta, GA 30303; [5]Department of Chemistry, Georgia State University, Atlanta, GA 30303; [6]Center for Molecular and Translational Medicine, Georgia State University, Atlanta, GA 30303.

* Maureen Meister and Hongwei Han are co-first authors.

**Correspondence to: Xiangming Ji, Ph. D. Email: xji4@gsu.edu.

Keywords: Fibrosis, ENDS (Electronic Nicotine Delivery Systems), COPD (Chronic obstructive pulmonary disease)

Abstract:

Background: Chronic obstructive pulmonary disease (COPD) is currently listed as the 3rd leading cause of death in the United States. COPD is marked by limitations in expiratory airflow, emphysematous destruction of the lungs, bronchitis, and chronic inflammation of the lung tissue. With the emerging prevalence in usage of electronic nicotine delivery systems (ENDS), the impact of ENDS on the development of lung diseases such as COPD requires further attention. Previous studies have shown that β-epithelial Na^+ channel (βENaC)- overexpressing mice have multiple emphysematous phenotypes, such as mucus accumulation and chronic inflammation. This study was aimed to elucidate the effects of e-cigarettes, a type of ENDS, on the development of COPD.

Methods: We hypothesized that acute repetitive usage of ENDS will exacerbate the features of COPD including mucus production, inflammation, and fibrosis, ultimately leading to lung injury. Twenty βENaC mice (10 mice per group) underwent whole body ENDS or sham air exposure for 2 hours daily over 10 days. Bronchoalveolar lavage (BAL) fluid and lung tissues were collected to assess for inflammation, fibrosis, mucus accumulation, and alveolar damage.

Results and Discussion: Our data showed that ENDS exposure significantly increased the alveolar size as compared with the control. We also found that level of inflammatory cytokines, such as CCL2, IL-13, and IL-10, were elevated in animals exposed to ENDS compared with control. Moreover, we observed ENDS exposure caused mucus accumulation, alveolar destruction, and fibrosis in the bronchioles of the βENaC mice. Additionally, ENDS exposure promoted apoptosis in pulmonary endothelial cell and epithelial cells.

Conclusion: Our data suggest that nicotine-containing e-cigarettes exacerbates features of COPD involving abnormal lung inflammation, mucus accumulation and apoptosis in βEnaC mice.

Background

Chronic obstructive pulmonary disease (COPD) is a primary leading cause of death with limited treatment options, accounting for more than 300 million deaths worldwide annually [1]. The phenotypes of COPD are characterized by limitations in expiratory airflow, emphysematous destruction of the lungs, chronic bronchitis, and inflammation of the lung tissue. Patients with COPD experience a variety of symptoms including shortness of breath, wheezing, and/or a chronic cough [2]. Cigarette smoking is a major risk factor for COPD. While cigarette smoking use in the U.S has decreased over the past 50 years, there has been a dramatic increase in the usage of electronic nicotine delivery systems (ENDS) as the substitutes[1]. As ENDS are perceived as a safer option compared to traditional cigarettes, they are often used to assist in cigarette smoking cessation. The risk of cigarette smoking and its contribution to chronic lung diseases has been well characterized, however, the health effects of ENDS are poorly known. [3]. Therefore, a thorough investigation into the effects of e-cigarette vapor on chronic lung conditions is essential.

ENDS include vape pens, hookah pens, electronic cigarettes (e-cigarettes or e-cigs), which transport noncombustible vaporized nicotine products to the lungs [4]. The common components of e-cigarette liquid include nicotine glycerin, propylene glycol, flavorings, and other ingredients. When heated, the nicotine-containing e-cigarette liquid generates vapor, which will be inhaled into the lungs. Vaporization of e-liquid generates toxic compounds similar to cigarette smoke. Reactive aldehydes, such as formaldehyde and acrolein, are common products from the thermal decomposition of propylene glycol and glycerol, the major vehicle components of e-liquids [5]. Notably, reactive aldehydes generated from ENDS have been noted in much greater concentrations than recommended occupational safety standards [6]. Accumulating data suggest that e-cigarette vapor induces oxidative stress and inflammation *in vitro* [7, 8] and *in vivo* [9, 10]. For example, e-cigarette liquid alone caused morphology changes in lung epithelial cells, by initiating a stress phenotype and inflammatory response [9]. As a major component of ENDS, nicotine, the addictive component in cigarettes and e-cigarettes, inhibits mucus hydration [11] and

induces pro-inflammatory dendritic cell responses [12]. Similar results were evidenced in mice where e-cigarette vapor induced airway responses similar to cigarette smoke, including airway inflammation, tissue remodeling, and enhanced mucin expression following four months of exposure [10]. These findings suggest the ability of nicotine-containing e-cigarettes could induce physiological changes akin to human COPD.

As the primary risk factor for COPD, cigarette smoking is widely used to study the pathogenesis of COPD in various animal models [13]. Despite the recent popularity of ENDS, there are limited investigations aimed at elucidating the effects of e-cigarettes on the development and progression of COPD [4]. Therefore, there is an unmet need to study the effects of ENDS, e-cigarettes in particular, on COPD progression utilizing the proper animal model with pre-existing phenotypes of COPD. In this study, we utilized the βENaC mouse, a transgenic line that exhibits defective airway mucus clearance due to the overexpression of the epithelial sodium channel non-voltage gated 1, beta subunit (*Scnn1b)* [14-16]. βENaC mice have been used in the investigation of respiratory diseases including COPD and cystic fibrosis [17, 18]. As this strain of mice has symptoms of emphysema and muco-obstruction [17], we postulated that ENDS could exacerbate the phenotypic response of COPD following acute e-cigarette vapor exposure. The specific goals of this study were to evaluate the effects of nicotine-containing e-cigarette vapor in the development and progression of a COPD phenotype including 1) inflammatory response in the lung tissues, 2) mucus accumulation within the bronchioles, 3) small airway fibrosis, and 4) the destruction and degradation of alveolar structure.

Methods

Animals and genotyping

Male and female βENaC were purchased from The Jackson Laboratory (congenic C57BL/6J background, Stock No. 006438, Bar Harbor, ME). Mice were housed in an environmentally

controlled animal facility and maintained on a 12 h light/dark cycle with free access to water and standard chow diet throughout treatment. All animal procedures described were approved by the Institutional Animal Care and Use Committee (IACUC) at Georgia State University. To have enough animals for this study, βENaC mice were bred with wild type C57BL/6J mice to produce an appropriate number of hemizygous βEnaC for our studies. Prior to weaning age, animals were genotyped to determine the presence *Scnn1b* overexpression. Briefly, tail snips were collected and lysed in Proteinase K overnight at 56°C in preparation for DNA extraction. DNA was extracted by Dneasy Blood and Tissue kit (Qiagen, Foster City, CA) in preparation for polymerase chain reaction (PCR). PCR was performed using primers specific for *Scnn1b* gene expression as suggested (Forward: CCTCCAAGAGTTCAACTACCG; Reverse: TCTACCAGCTCAGCCACAGTG) [16]. To verify the expression of *Scnn1b* gene, samples were run on a 4% agarose gel containing ethidium bromide. Mice identified as possessing *Scnn1b* overexpression were tagged as βENaC mice for future studies.

ENDS exposure to βENaC mice

At 12-weeks of age, mice (n=10, five male and five female per group) were randomized into either ENDS exposure group or the control group (sham air). Mice in the ENDS group were exposed to e-cigarette vapor for 1-hour twice daily at a frequency of 5 times per week for a total duration of 10 days as shown in Fig. 1A**.** Mice were placed in a smoking chamber attached to an inExpose Smoking Robot (SCIREQ, Montreal, QC, Canada) with an attached e-cigarette accessory (ECX JoyeTech E-Vic Mini, SCIREQ, Canada) for the administration of vaporized S brand e-cigarette liquid containing nicotine at 50 mg/ml. After 10-days of e-cigarette vapor exposure, animals were euthanized within 24 h after last e-cigarette vapor exposure using CO_2. Serum, bronchoalveolar lavage (BAL) fluid, and lung tissues were collected for analysis as described below.

Bronchoalveolar lavage fluid and cytokine measurements

After the mice were euthanized, tracheostomy was performed and lungs were immediately flushed with 1 mL ice-cold phosphate buffered saline (PBS) twice for collection of BAL fluid. Blood was collected via the abdominal aorta, allowed to sit for 30 min to promote coagulation and centrifuged at 5,000 rpm for 10 min for isolation of serum. Total cells from the BAL were centrifuged and counted using Countess™ II Automated Cell Counter (Invitrogen, Carlsbad, CA) as previously described [16]. Differential immune cell count (5,000 cells/slide) was performed on Shandon cytospin slides (Thermo Shandon, Pittsburgh, PA) stained with Diff-Quik (Dade Bering, Newark, DE). The BAL supernatant and serum samples were stored at -80°C until analysis. Expression of inflammatory cytokines, proteases, and growth factors was assessed in BAL fluid via Mouse XL Cytokine Array (R&D Systems, Minneapolis, MN) following manufacturer's instructions to determine the presence of a localized inflammatory response within the lung.

Morphometric assessment

In order to determine the effects of ENDS exposure on the development of emphysema, we did a morphometric assessment according to the previous protocol [17, 19]. Briefly, the mouse lungs were inflated with 1% low melting-point agarose to 25 cm of fixative pressure. After 48 hours fixation, lungs were paraffin-embedded, sectioned and stained with hematoxylin and eosin (H&E). Mean linear intercepts were determined and calculated [20].

Immunohistochemical and histology analysis.

The mouse lungs were inflated with 1% low melting-point agarose to 25 cm of fixative pressure and then fixed with 4% neutral buffered formalin for 48 hours. Later, these tissue samples were embedded in paraffin, and sectioned into 4 μm sections using a rotary microtome. For immunohistochemical analysis, tissue sections were dewaxed with xylene and rehydrated with graded concentrations of ethanol, followed by antigen retrieval in 10 mM citric acid solution (pH =

6) for 20 min using a pressure cooker. Endogenous peroxidase activity was blocked by 3% hydrogen peroxide. After blocking with 5% BSA for 30 min, the slides were incubated with the primary antibodies against the following proteins at 4°C overnight: α smooth muscle actin (α-SMA) 1:500 (Ab5694; Abcam); Von Willebrand Factor (vWF) 1:300 (A008229; Agilent). After washing, the sections were incubated with the appropriate HRP polymers and developed with 3-3′ diaminobenzidine solution (DAB substrate kit; Vector Laboratories). After counterstaining with hematoxylin, the slides were dehydrated and mounted with a mounting medium.

For Hematoxylin and Eosin (H&E) staining, the paraffin slides were baked at 60℃ for 2 hours, then dewaxed with xylene and rehydrated with graded ethanol solutions. Next, the slides were incubated with Mayer's Hematoxylin for 10 min and washed under tap water for 10 min. Slides were then immersed in Eosin for 30 sec and washed under tap water, after which, the slides were dehydrated and mounted with a mounting medium.

Periodic-acid Schiff (PAS; Sigma Aldrich, Saint Louis, MO) staining was used to evaluate mucus accumulation and immune cell infiltration. Masson's Trichrome (Sigma, St. Louis, MO) and Picro-Sirius Red (Abcam, Cambridge, MA) staining were used to assess collagen deposition in lung tissue. All stainings were performed following the manufacturers' instructions. All images were taken at 20x magnification using Keyence Fluorescent Microscope (Keyence, Itasca, IL).

Cell Culture

Human airway epithelial cells (16HBE) were a gift from Dr. Pierre Massion (Vanderbilt University) and maintained in DMEM media. 16HBE cells were grown in 1% penicillin/streptomycin with 10% fetal bovine serum. Human Aortic Endothelial Cells (HAEC) were obtained from Invitrogen (Invitroen, Carlsbad, CA) and cultured in endothelial cell growth medium supplemented with low-serum (2% V/V FBS) (PromoCell; Heidelberg, Germany), and both cells were maintained in a cell culture incubator at 37℃ and 5% CO_2. 16HBE cells were plated at 30,000 cells/well in 6-well plates. Then cells were treated with e-cigarette liquid with nicotine (50 mg/ml) or e-cigarette liquid

without nicotine for 48 hours and harvested for analysis of protein expression by western blot. Similarly, HAEC cells were cultured in 6-well plates at a density of 2.0×10^5 cells/well, starved overnight, and treated with e-cigarette liquid with nicotine (50 mg/ml), or e-cigarette liquid without nicotine for 24 hours or 1 mM H_2O_2 for 12 hours (positive control) and then subjected to Annexin V/PI apoptosis analysis by flow cytometry.

Annexin V/PI apoptosis detection with flow cytometry.

The cells were detached with accutase solution and washed with PBS and later binding buffer, followed by resuspension in binding buffer at 10^6 cells/ml. The cell suspensions were incubated with 5 µL of FITC-conjugated Annexin V (V13242, Thermo) for 15 min at room temperature without exposure to light, followed by washing and resuspension in binding buffer. Propidium Iodide was added followed by incubation for 5 min. The cells were acquired using LSRFortessa flow cytometer (BD Biosciences, Durham, NC), and the data analyzed by FlowJo software (BD, Durham, NC).

TUNEL Assay for apoptosis detection.

TUNEL assay was performed using VasoTACS™ In Situ Apoptosis Detection Kit (4826-30-K, Trevigen, Gaithersburg, MD) following the manufacturer's instructions. In brief, after rehydration, tissue slides were incubated with Proteinase K Solution for 20 min at room temperature, followed by quenching for 5 min. 50 µL of Labeling Reaction Mix were added to the tissues and the slides were incubated at 37℃ for 60 min, after which the reaction was terminated by adding the stop solution. The slides were covered with Strep-HRP Solution for another 10 min and developed using TACS Blue Label solution. After counterstaining by Red Counterstain C, slides were dehydrated and mounted with mounting medium.

Data analysis.

In the case of only two groups, two-tail *t*-tests were performed to assess the differences. All analyses were carried out using Prism7.0 software (GraphPad Software Inc., San Diego, CA). Values are represented as mean ± SEM. Levels of significance designated as $p < 0.05$ unless otherwise indicated.

Results

βENaC mice characteristics.

Results of genotyping were used to dictate the use of animals in the treatment procedure as shown in Fig. 1A. Elevated levels of immune cells, specifically neutrophils, have been associated with COPD progression and exacerbation [21, 22]. Previous studies have demonstrated that βENaC mice have a higher mucin expression and persistent increases in neutrophils and macrophages [16, 17]. These phenotypes indicate an active immune status in the lungs of these animals before e-cigarette exposure, which could be a model to explore the effects of ENDs on the development of COPD.

ENDS exposure induces airspace enlargement and mucus accumulation in the lungs.

COPD is distinguished by airway remodeling, mucus accumulation, goblet cell metaplasia, and inflammation [23]. We first measured the airspace enlargement, which are the characteristics of COPD, in βENaC mice exposed to air or ENDs. As shown in Fig. 1B and 1C, ENDs exposure significantly induced the airspace enlargement compared with the sham air control in βEnaC mice. These data suggest acute ENDS exposure impairs the alveolar structure in βEnaC mice.

Because βENaC mice exhibit mucus accumulation due to dehydration in the airway epithelium [16], these strain of mice are known as a model of muco-obstructive lung disease for the investigation of COPD [15]. Airway mucus content was evaluated histologically using PAS staining [16]. As mucus accumulation is a feature of COPD, we therefore asked if ENDS exposure

could further induce airway mucus accumulation and progress the development of COPD. As shown in Fig. 1D, ENDS exposure increased the deposition of mucus in the bronchioles compared with control. Goblet cells are the primary cell type for mucus production, and goblet cell metaplasia commonly occurs in association with exposure to cigarette smoke in animals models [24]. Although goblet cells are not prevalent in all the animal models, a previous study found goblet cell metaplasia as well as epithelial cell hypertrophy exist in the βENaC mice [17]. Goblet cell metaplasia is marked by the accumulation of goblet cells in the epithelium lining of the bronchiole and responsible for tissue regeneration. Because goblet cells are the cells primarily responsible for mucus production [25], our data suggest the ENDS exposure causes mucus overproduction by activating goblet cell metaplasia in the lung.

ENDs exposure causes immune cells infiltration and inflammation in the lungs

The dysregulation of immune cells, especially the elevated presence of neutrophils is known to cause the goblet cell metaplasia [26]. In order to profile the involvement of different immune cells, we then performed the Diff-Quik staining on the cells from the BAL. As shown in Fig. 2A and 2B, we found ENDS exposure causes increased infiltration of immune cells including macrophages and neutrophils in βENaC mice as compared with the control.

To elucidate the effects of ENDS exposure on airway inflammation, we performed mice cytokine arrays using BAL supernatant from the experimental mice. As shown in Fig. 2C, increased expression of a multitude of inflammatory cytokines was seen in the BAL fluid of βENaC mice prior to ENDS exposure by comparing the pixel density (Image J, NIH, MA) of individual cytokines. Following ENDS exposure, inflammatory cytokines such as CCL2 ($p<0.01$), IL-13 ($p<0.0001$), IL-10 ($p=0.0073$,), M-CSF ($p<0.01$) concentrations were significantly higher in comparison with sham air control (Fig. 2E-G). CCL-2, IL-10, and IL-13 have been indicated in contributing to macrophage infiltration, M2 macrophage polarization, and pulmonary fibrosis [27-

29]. Thus, these results indicate ENDS exposure contribute to immune cell infiltration such as macrophages and neutrophils as well as inflammatory cytokines productions within the airway in the βENaC mice.

ENDs exposure promotes exacerbation of small airway fibrosis.

Small airway fibrosis is considered an early feature of COPD. High-resolution computerized tomography (HRCT) suggest that small airway remodeling is the earliest feature of COPD and could be used to determine the trajectory of disease progression [30]. Recent study showed that e-cigarette vapor exposure promotes fibroblast differentiation to myofibroblasts, which leads synthesis of abnormal amounts of extracellular matrix (ECM) proteins and fibrosis [31-33]. Other evidence points out that chronic nicotine-containing e-cigarette vapor exposure causes multi-organ fibrosis in mice [34]. Airway remodeling involves multiple physiological changes in the lung such as thickening of the airway wall, goblet cell hyperplasia, mucous gland hypertrophy, the luminal obstruction caused by inflammatory exudates [35]. Moreover, destruction and fibrosis of the alveolar wall with the deposition of ECM uniquely occurs in patients with COPD rather than in patients with other respiratory conditions, such as asthma [36, 37]. Therefore, we examined the effects of ENDS on the progression of fibrosis in this animal model. We assessed the deposition of collagen, a major constituent in ECM within lung tissue following exposure to ENDS. Picro-Sirius red (Fig. 3A) was used to stain for all types of collagen in the lung tissue of βENaC mice with and without ENDS exposure. As shown Fig. 3A, 10-day exposure to ENDS elevated collagen deposition in βENaC mice within the airway and lung parenchyma (Fig. 3A bottom panel) compared with the control (Fig. 3A top panel). Quantitative analysis of Picro-Sirius red staining was shown in Fig. 3B. These results were confirmed by Masson's Trichrome staining (Fig. 3C). In addition, small airway destruction was also observed in mice upon ENDS exposure (Fig. 3A, bottom panel) compared with the control (Fig. 3A, top panel).

Myofibroblasts, the activated form of fibroblasts, contribute to ECM deposition and therefore are responsible for small airway fibrosis within the lung [38]. As myofibroblasts specially express the protein α-SMA, IHC staining of α-SMA was used to evaluate the presence of fibrotic tissue in the lung interstitium. As shown in the top panel of Fig. 3E**,** ENDS exposure elevated the expression α-SMA in the subpleural and interspersed in the parenchyma of βENaC mice compared with the control (Fig. 3C, bottom panel). These results are supported by a previous study showed that chronic exposure to nicotine-containing ENDS caused fibrosis in kidney and heart tissue [34]. These data suggest that exposure to nicotine-containing ENDS induces ECM deposition, and therefore fibrosis within the lung tissue, which is responsible for lung tissue remodeling by the activation of myofibroblasts.

ENDS exposure causes lung vascular injury by inducing lung endothelial cell apoptosis

Vascular cell dysfunction and death are the primary phenotypes in cigarette smoking-related lung diseases [39]. Newly emerging evidence suggests ENDS exposure induces endothelial inflammation [40] and oxidative stress [41]. Therefore, we examined the effect of ENDS on vascular injury in the lungs. Pulmonary endothelial cell apoptosis has been known to promote the progression of emphysema [42]. Thus, we hypothesized that ENDS exposure would lead to the apoptosis of pulmonary endothelial cells. Using TUNEL staining, we were able to detect apoptosis in the fixed lung tissues. Consistent with the pattern from the positive control, we found ENDS exposure leads to the elevation of apoptosis in pulmonary endothelial cells (Fig. 4A bottom, black dots indicated by green arrows) whereas the apoptosis was barely seen in the control (Fig. 4A Top). Quantitative analysis of TUNEL staining from βENaC mice without and with e-cigarette vapor exposure was shown in Fig. 4B.

In order to confirm the death of endothelial cells, we also performed immunohistochemical staining of von Willebrand Factor (vWF), a widely-used biomarker for vascular endothelial cells in the lungs of mice without or with ENDS exposure. We observed that ENDS exposure significantly

diminished the amount of vWF positive endothelial cells compared with the control (Fig. 4C and 4D).

Based on the results obtained *in vivo*, we further employed the HAEC cells to test the effects of ENDS *in vitro*. As shown in Fig. 5F, exposure to nicotine-containing e-cigarette liquids (Fig. 5F bottom right, 57%), significantly decreased the cell viability compared with the control (Fig. 5F top left, 82%). Interestingly, a significant toxic effect of e-cigarette liquid exposure without nicotine (Fig. 5F bottom left, 75%) was also observed as shown in Fig. 5F bottom left and 5E. Thus, these data suggest that ENDS exposure, particularly nicotine-containing e-cigarette liquid, causes lung vascular injury by inducing lung endothelial cell apoptosis.

ENDS exposure causes apoptosis in lung epithelial cells

COPD consists of chronic bronchitis and emphysema, in which alveolar destruction leads to impaired air exchange [43]. Previous study showed that βENaC mice spontaneously develop an emphysematous phenotype, and chronic e-cigarette exposure causes alveolar destruction in a nicotine-dependent manner [10]. We, therefore, tested whether nicotine-containing e-cigarette vapor exposure could cause alveolar destruction. As expected, we detected apoptosis in the fixed lung tissues by using TUNEL staining. Consistent with the pattern shown in endothelial cells, we found ENDS exposure leads to the elevation of apoptosis in airway epithelial cells (Fig. 5A bottom, black dots indicated by green arrows) compared to the control (Fig. 5A top). Quantitative analysis of TUNEL staining from βENaC mice without and with e-cigarette vapor exposure was shown in Fig. 5B. We then validated the data in *vitro* by culture of airway epithelial cells (16HBE) with e-cigarette liquid. As shown in Fig. 5C and 5D, e-cigarette liquid with nicotine and without nicotine significantly leads the cell death compared with the control. Altogether, our results suggested that ENDS exposure leads to epithelium damage and remodeling by causing apoptosis in lung epithelium.

Discussion

Cigarette smoking is considered the major risk factor for the development of lung diseases such as COPD and lung cancer in the developed world. The toxic effects of smoking are attributed to the notorious mixture of oxidants, irritants, and carcinogens. Based on the assumption that ENDS vapor containing fewer toxins than conventional cigarette smoke, they were initially considered to be safer [44, 45]. While ENDS have a less detrimental effect in terms of environmental pollutants [46] and production of carcinogens [47], the health effects of ENDS usage on chronic lung conditions, such as COPD, and associated public health recommendations remain scant.

Recent data classified ENDS aerosol is unsafe, as it contains heavy metals such as nickel and chromium, volatile organic, and carcinogen compounds such as acrolein and crotonaldehyde [45, 48]. Results from cell culture and animal studies suggest nicotine is the driving force of emphysema, lung tissue inflammation, and airway surface dehydration [10]. However, differences in heating elements, humectants, and flavorings have also been shown to produce different physiological responses in terms of reactive oxygen species (ROS) production [9]. In addition, ENDS users often combine e-cigarette liquid with tetrahydrocannabinol (THC) and cannabidiol (CBD) for vaping, potentially worsening the effects [49]. By February of 2020, the Centers for Disease Control and Prevention reported approximately 3,000 hospitalizations associated with e-cigarette or vaping, product use–associated lung injury (EVALI) [50]. Given the clinical health issues of ENDS in lung pathobiology, our current study was to investigate the effects of ENDS on pro-inflammatory and pro-fibrotic phenotypes *in vivo* and *in vitro*.

In this present study, an animal model with pre-existing phenotypes of COPD was used to determine the effect of ENDS on the progression and exacerbation of COPD. Following a 10-day acute exposure to nicotine-containing e-cigarette vapor, significant mucus accumulation was noted within the bronchioles of βENaC mice as evidenced by PAS staining. Given the phenotypes of this transgenic line, mucus accumulation was expected and was exacerbated by ENDS vapor

exposure. Nicotine is not only the addictive component of cigarettes, but is also a key factor in the initiation and progression of COPD and is known to hinder the hydration of mucus [12]. Cigarette smoke generated from high-dose nicotine cigarettes induced more emphysematous changes than low-dose nicotine cigarettes in elastase-treated rats [54]. Similarly, an *in vitro* study showed that nicotine induced mucus production in bronchial cells [55]. Consistent with these data, our results indicated that mucus accumulation occurs in the lungs of βENaC mice following exposure to nicotine-containing ENDS vapor (Fig. 1D). Reactive aldehydes, such as formaldehyde and acrolein, are common products from the thermal decomposition of propylene glycol and glycerol, the major vehicle components of e-liquids [5]. In addition, popular sweet and creamy flavors used in e-liquids containing dicarbonyls such as diacetyl and 2,3-pentanedione could also cause significant pulmonary epithelial apoptosis and inflammation in animal models [51, 52]. These reactive carbonyls generated from flavors have been noted in much greater concentrations than occupational safety standards [6]. Inhalation of high levels of volatile butter flavoring (2,3-butanedione, an alpha-diketone) could cause bronchiolitis obliterans [53]. Although flavored ENDS aerosols have lower levels of toxins than tobacco smoke, inhalation of ENDS aerosols will cause the accumulation of carbonyls in the circulation [54], which may be detrimental to the endothelium. Our results support the role of nicotine in the progression of muco-obstructive conditions. However, further studies are needed to compare the pulmonary consequences of inhaled nicotine with different flavorings and the potential for dose dependent responses.

As expected, ENDS vapor exposure increases immune cell infiltration and pro-inflammatory cytokines production within BAL fluid. Most notably, CCL2, also known as monocyte chemotactic/chemoattractant protein 1 (MCP1), is a soluble factor in driving monocytic infiltration of tissues during inflammatory processes [55]. In a previous study, CCL2-producing macrophages are highly activated in patients with COPD, which is associated with increased monocyte migration [55]. Additionally, significant increases in IL-10, a regulatory anti-inflammatory cytokine, was also observed in response to ENDS exposure. Elevation of IL-10 was shown to be present

with other pro-inflammatory cytokines, although the presence of IL-10 may negatively regulate these pro-inflammatory cytokines [50]. In addition, IL-10 is known to coincide with the switching of macrophages towards the M2-like phenotype in patients with COPD [27]. Similar to IL-10, IL-13 was also observed increased upon ENDS exposure, another cytokine known to induce M2-macrophage polarization [28]. Given that the attenuation of M2-macrophages slows the progression of pulmonary fibrosis [29], these data suggested M2-macrophages play an important role during the development of COPD in our animal model.

We premised that ENDS exposure might cause the elevation of inflammatory markers indicates inflammation and pro-fibrotic response. As seen in Fig. 3A and C, ENDS vapor exposure caused collagen deposition within the lung tissues. In addition, we also found e-cigarette vapor containing nicotine caused a significant increase in the expression of α-SMA (Fig. 3E), suggesting activation of fibroblasts and the fibrotic phenotype in our animal model. The detailed mechanism in which ENDS contributes to lung tissue damage is worth further investigation.

While the majority of research focus is on the epithelial lining within the airway, recent evidence suggests endothelial dysfunction plays an essential role in the oxidative stress response to e-cigarette vapor [41]. Here, we validated the effects of ENDS exposure on the cell viability of endothelial cells (HAEC) and epithelial cells (16HBE) via flow cytometry. Cell viability was significantly decreased following treatment with e-cigarette liquid containing nicotine (Fig. 4F and 5C). Interestingly, e-cigarette liquid without nicotine did not have the same effect on cell death and viability remained comparable to control, suggesting nicotine plays a significant role in apoptosis of endothelial and epithelial cells responsive to inflammation and oxidative stress. We also found e-cigarette liquid without nicotine affect the cell viability, indicating other components of e-cigarette could be toxic to endothelial cells as well. A recent study found that chronic ENDS exposure without nicotine adversely affect the vascular endothelial network by promoting oxidative stress and immune cell adhesion [41]. Further investigation is needed to elucidate the impact of chronic ENDS exposure without nicotine on the endothelium within the lung.

Conclusion

Taken together, our results demonstrate nicotine-containing ENDS, in the form of e-cigarette vapor, causes the exacerbation of features of COPD in βENaC-overexpressing mice. Specifically, acute exposure to nicotine-containing e-cigarette vapor results in mucus accumulation, overproduction of inflammatory cytokines, deposition of ECM, and fibrosis. Last but not the least, e-cigarette exposure induces cell death in epithelium and endothelium in the lung of βENaC-overexpressing mice.

Ethics approval:

All animal procedures described were approved by the Institutional Animal Care and Use Committee (IACUC) at Georgia State University.

Consent for publication

All the authors have approved to the material to be submitted to the journal of inflammation.

Availability of data and materials

All data are available from the corresponding author on request.

Competing interests

The authors declare that they have no competing interests.

Authors' contributions

MM, HH and XJ planned and designed experiments and wrote the manuscript. MM carried out the animal studies performed molecular and cell biology experiments. MM, HH, GP, and JA acquired histology analysis. VN and GP performed flow cytometry and FACs analysis. MM, HH, and OO assisted with animal studies. TD, JY, MZ, ZL, and XJ provided intellectual oversight and reviewed the manuscript. PS provided pathological support and statistical analyses.

Acknowledgment

We thank Dr. Jian-dong Li (Georgia State University) for useful discussions.

Funding:

This work was supported by FAMRI foundation YFEL141014 to XJ.

This work was also supported by R42AA112713 from NIH to JY

Reference:

1. Barnes PJ, Shapiro SD, Pauwels RA: **Chronic obstructive pulmonary disease: molecular and cellular mechanisms.** *Eur Respir J* 2003, **22:**672-688.
2. U.S. Department of Health and Human Services: **E-cigarette use among youth and young adults: A report of the surgeon general.** 2016,.
3. Vij N, Chandramani-Shivalingappa P, Van Westphal C, Hole R, Bodas M: **Cigarette smoke-induced autophagy impairment accelerates lung aging, COPD-emphysema exacerbations and pathogenesis.** *Am J Physiol Cell Physiol* 2018, **314:**C73-C87.
4. Reidel B, Radicioni G, Clapp PW, Ford AA, Abdelwahab S, Rebuli ME, Haridass P, Alexis NE, Jaspers I, Kesimer M: **E-Cigarette Use Causes a Unique Innate Immune Response in the Lung, Involving Increased Neutrophilic Activation and Altered Mucin Secretion.** *Am J Respir Crit Care Med* 2018, **197:**492-501.
5. Ogunwale MA, Li M, Ramakrishnam Raju MV, Chen Y, Nantz MH, Conklin DJ, Fu XA: **Aldehyde Detection in Electronic Cigarette Aerosols.** *ACS Omega* 2017, **2:**1207-1214.
6. Khlystov A, Samburova V: **Flavoring Compounds Dominate Toxic Aldehyde Production during E-Cigarette Vaping.** *Environ Sci Technol* 2016, **50:**13080-13085.
7. Bahl V, Lin S, Xu N, Davis B, Wang YH, Talbot P: **Comparison of electronic cigarette refill fluid cytotoxicity using embryonic and adult models.** *Reprod Toxicol* 2012, **34:**529-537.
8. Farsalinos KE, Romagna G, Allifranchini E, Ripamonti E, Bocchietto E, Todeschi S, Tsiapras D, Kyrzopoulos S, Voudris V: **Comparison of the cytotoxic potential of cigarette smoke and electronic cigarette vapour extract on cultured myocardial cells.** *Int J Environ Res Public Health* 2013, **10:**5146-5162.
9. Lerner CA, Sundar IK, Yao H, Gerloff J, Ossip DJ, McIntosh S, Robinson R, Rahman I: **Vapors produced by electronic cigarettes and e-juices with flavorings induce toxicity, oxidative stress, and inflammatory response in lung epithelial cells and in mouse lung.** *PLoS One* 2015, **10:**e0116732.
10. Garcia-Arcos I, Geraghty P, Baumlin N, Campos M, Dabo AJ, Jundi B, Cummins N, Eden E, Grosche A, Salathe M, Foronjy R: **Chronic electronic cigarette exposure in mice induces features of COPD in a nicotine-dependent manner.** *Thorax* 2016, **71:**1119-1129.
11. Chen EY, Sun A, Chen CS, Mintz AJ, Chin WC: **Nicotine alters mucin rheological properties.** *Am J Physiol Lung Cell Mol Physiol* 2014, **307:**L149-157.
12. Vassallo R, Kroening PR, Parambil J, Kita H: **Nicotine and oxidative cigarette smoke constituents induce immune-modulatory and pro-inflammatory dendritic cell responses.** *Mol Immunol* 2008, **45:**3321-3329.
13. Serban KA, Petrache I: **Mouse Models of COPD.** *Methods Mol Biol* 2018, **1809:**379-394.
14. Lewis BW, Sultana R, Sharma R, Noel A, Langohr I, Patial S, Penn AL, Saini Y: **Early Postnatal Secondhand Smoke Exposure Disrupts Bacterial Clearance and Abolishes Immune Responses in Muco-Obstructive Lung Disease.** *J Immunol* 2017, **199:**1170-1183.
15. Livraghi-Butrico A, Grubb BR, Wilkinson KJ, Volmer AS, Burns KA, Evans CM, O'Neal WK, Boucher RC: **Contribution of mucus concentration and secreted mucins Muc5ac and Muc5b to the pathogenesis of muco-obstructive lung disease.** *Mucosal Immunol* 2017, **10:**395-407.
16. Mall M, Grubb BR, Harkema JR, O'Neal WK, Boucher RC: **Increased airway epithelial Na+ absorption produces cystic fibrosis-like lung disease in mice.** *Nat Med* 2004, **10:**487-493.
17. Mall MA, Harkema JR, Trojanek JB, Treis D, Livraghi A, Schubert S, Zhou Z, Kreda SM, Tilley SL, Hudson EJ, et al: **Development of chronic bronchitis and emphysema in**

beta-epithelial Na+ channel-overexpressing mice. *Am J Respir Crit Care Med* 2008, **177:**730-742.
18. Gehrig S, Duerr J, Weitnauer M, Wagner CJ, Graeber SY, Schatterny J, Hirtz S, Belaaouaj A, Dalpke AH, Schultz C, Mall MA: **Lack of neutrophil elastase reduces inflammation, mucus hypersecretion, and emphysema, but not mucus obstruction, in mice with cystic fibrosis-like lung disease.** *Am J Respir Crit Care Med* 2014, **189:**1082-1092.
19. Bartalesi B, Cavarra E, Fineschi S, Lucattelli M, Lunghi B, Martorana PA, Lungarella G: **Different lung responses to cigarette smoke in two strains of mice sensitive to oxidants.** *Eur Respir J* 2005, **25:**15-22.
20. Dunnill MS: **Quantitative methods in the study of pulmonary pathology.** *Thorax* 1962, **17:**320-328.
21. Stanescu D, Sanna A, Veriter C, Kostianev S, Calcagni PG, Fabbri LM, Maestrelli P: **Airways obstruction, chronic expectoration, and rapid decline of FEV1 in smokers are associated with increased levels of sputum neutrophils.** *Thorax* 1996, **51:**267-271.
22. Gompertz S, O'Brien C, Bayley DL, Hill SL, Stockley RA: **Changes in bronchial inflammation during acute exacerbations of chronic bronchitis.** *Eur Respir J* 2001, **17:**1112-1119.
23. Gorska K, Krenke R, Kosciuch J, Korczynski P, Zukowska M, Domagala-Kulawik J, Maskey-Warzechowska M, Chazan R: **Relationship between airway inflammation and remodeling in patients with asthma and chronic obstructive pulmonary disease.** *Eur J Med Res* 2009, **14 Suppl 4:**90-96.
24. Kato K, Chang EH, Chen Y, Lu W, Kim MM, Niihori M, Hecker L, Kim KC: **MUC1 contributes to goblet cell metaplasia and MUC5AC expression in response to cigarette smoke in vivo.** *Am J Physiol Lung Cell Mol Physiol* 2020.
25. Ramos FL, Krahnke JS, Kim V: **Clinical issues of mucus accumulation in COPD.** *Int J Chron Obstruct Pulmon Dis* 2014, **9:**139-150.
26. Yanagihara K, Seki M, Cheng PW: **Lipopolysaccharide Induces Mucus Cell Metaplasia in Mouse Lung.** *Am J Respir Cell Mol Biol* 2001, **24:**66-73.
27. Metcalfe HJ, Lea S, Hughes D, Khalaf R, Abbott-Banner K, Singh D: **Effects of cigarette smoke on Toll-like receptor (TLR) activation of chronic obstructive pulmonary disease (COPD) macrophages.** *Clin Exp Immunol* 2014, **176:**461-472.
28. Shaykhiev R, Krause A, Salit J, Strulovici-Barel Y, Harvey BG, O'Connor TP, Crystal RG: **Smoking-dependent reprogramming of alveolar macrophage polarization: implication for pathogenesis of chronic obstructive pulmonary disease.** *J Immunol* 2009, **183:**2867-2883.
29. Yao Y, Wang Y, Zhang Z, He L, Zhu J, Zhang M, He X, Cheng Z, Ao Q, Cao Y, et al: **Chop Deficiency Protects Mice Against Bleomycin-induced Pulmonary Fibrosis by Attenuating M2 Macrophage Production.** *Mol Ther* 2016, **24:**915-925.
30. Barnes PJ: **Small airway fibrosis in COPD.** *Int J Biochem Cell Biol* 2019, **116:**105598.
31. Grody WW, Cutting GR, Klinger KW, Richards CS, Watson MS, Desnick RJ, Subcommittee on Cystic Fibrosis Screening AoGSCAACoMG: **Laboratory standards and guidelines for population-based cystic fibrosis carrier screening.** *Genet Med* 2001, **3:**149-154.
32. Gerloff J, Sundar IK, Freter R, Sekera ER, Friedman AE, Robinson R, Pagano T, Rahman I: **Inflammatory Response and Barrier Dysfunction by Different e-Cigarette Flavoring Chemicals Identified by Gas Chromatography-Mass Spectrometry in e-Liquids and e-Vapors on Human Lung Epithelial Cells and Fibroblasts.** *Appl In Vitro Toxicol* 2017, **3:**28-40.

33. Zahedi A, Phandthong R, Chaili A, Remark G, Talbot P: **Epithelial-to-mesenchymal transition of A549 lung cancer cells exposed to electronic cigarettes.** *Lung Cancer* 2018, **122:**224-233.
34. Crotty Alexander LE, Drummond CA, Hepokoski M, Mathew D, Moshensky A, Willeford A, Das S, Singh P, Yong Z, Lee JH, et al: **Chronic inhalation of e-cigarette vapor containing nicotine disrupts airway barrier function and induces systemic inflammation and multiorgan fibrosis in mice.** *Am J Physiol Regul Integr Comp Physiol* 2018, **314:**R834-R847.
35. Aoshiba K, Nagai A: **Differences in airway remodeling between asthma and chronic obstructive pulmonary disease.** *Clin Rev Allergy Immunol* 2004, **27:**35-43.
36. Keglowich LF, Borger P: **The Three A's in Asthma - Airway Smooth Muscle, Airway Remodeling & Angiogenesis.** *Open Respir Med J* 2015, **9:**70-80.
37. Mauad T, Bel EH, Sterk PJ: **Asthma therapy and airway remodeling.** *J Allergy Clin Immunol* 2007, **120:**997-1009; quiz 1010-1001.
38. Lomas NJ, Watts KL, Akram KM, Forsyth NR, Spiteri MA: **Idiopathic pulmonary fibrosis: immunohistochemical analysis provides fresh insights into lung tissue remodelling with implications for novel prognostic markers.** *Int J Clin Exp Pathol* 2012, **5:**58-71.
39. Anderson C, Majeste A, Hanus J, Wang S: **E-Cigarette Aerosol Exposure Induces Reactive Oxygen Species, DNA Damage, and Cell Death in Vascular Endothelial Cells.** *Toxicol Sci* 2016, **154:**332-340.
40. Schweitzer KS, Chen SX, Law S, Van Demark M, Poirier C, Justice MJ, Hubbard WC, Kim ES, Lai X, Wang M, et al: **Endothelial disruptive proinflammatory effects of nicotine and e-cigarette vapor exposures.** *American journal of physiology Lung cellular and molecular physiology* 2015, **309:**L175-L187.
41. Chatterjee S, Tao JQ, Johncola A, Guo W, Caporale A, Langham MC, Wehrli FW: **Acute exposure to e-cigarettes causes inflammation and pulmonary endothelial oxidative stress in nonsmoking, healthy young subjects.** *Am J Physiol Lung Cell Mol Physiol* 2019, **317:**L155-L166.
42. Petrache I, Fijalkowska I, Medler TR, Skirball J, Cruz P, Zhen L, Petrache HI, Flotte TR, Tuder RM: **alpha-1 antitrypsin inhibits caspase-3 activity, preventing lung endothelial cell apoptosis.** *Am J Pathol* 2006, **169:**1155-1166.
43. Barnes PJ: **Cellular and molecular mechanisms of chronic obstructive pulmonary disease.** *Clin Chest Med* 2014, **35:**71-86.
44. Hua M, Talbot P: **Potential health effects of electronic cigarettes: A systematic review of case reports.** *Prev Med Rep* 2016, **4:**169-178.
45. Margham J, McAdam K, Forster M, Liu C, Wright C, Mariner D, Proctor C: **Chemical Composition of Aerosol from an E-Cigarette: A Quantitative Comparison with Cigarette Smoke.** *Chem Res Toxicol* 2016, **29:**1662-1678.
46. Schober W, Szendrei K, Matzen W, Osiander-Fuchs H, Heitmann D, Schettgen T, Jorres RA, Fromme H: **Use of electronic cigarettes (e-cigarettes) impairs indoor air quality and increases FeNO levels of e-cigarette consumers.** *Int J Hyg Environ Health* 2014, **217:**628-637.
47. Czogala J, Goniewicz ML, Fidelus B, Zielinska-Danch W, Travers MJ, Sobczak A: **Secondhand exposure to vapors from electronic cigarettes.** *Nicotine Tob Res* 2014, **16:**655-662.
48. Aherrera A, Olmedo P, Grau-Perez M, Tanda S, Goessler W, Jarmul S, Chen R, Cohen JE, Rule AM, Navas-Acien A: **The association of e-cigarette use with exposure to nickel and chromium: A preliminary study of non-invasive biomarkers.** *Environ Res* 2017, **159:**313-320.

49. Layden JE, Ghinai I, Pray I, Kimball A, Layer M, Tenforde MW, Navon L, Hoots B, Salvatore PP, Elderbrook M, et al: **Pulmonary Illness Related to E-Cigarette Use in Illinois and Wisconsin - Final Report.** *N Engl J Med* 2020, **382:**903-916.
50. Blount BC, Karwowski MP, Shields PG, Morel-Espinosa M, Valentin-Blasini L, Gardner M, Braselton M, Brosius CR, Caron KT, Chambers D, et al: **Vitamin E Acetate in Bronchoalveolar-Lavage Fluid Associated with EVALI.** *N Engl J Med* 2020, **382:**697-705.
51. Hubbs AF, Cumpston AM, Goldsmith WT, Battelli LA, Kashon ML, Jackson MC, Frazer DG, Fedan JS, Goravanahally MP, Castranova V, et al: **Respiratory and olfactory cytotoxicity of inhaled 2,3-pentanedione in Sprague-Dawley rats.** *Am J Pathol* 2012, **181:**829-844.
52. Morgan DL, Jokinen MP, Price HC, Gwinn WM, Palmer SM, Flake GP: **Bronchial and bronchiolar fibrosis in rats exposed to 2,3-pentanedione vapors: implications for bronchiolitis obliterans in humans.** *Toxicol Pathol* 2012, **40:**448-465.
53. Kreiss K, Gomaa A, Kullman G, Fedan K, Simoes EJ, Enright PL: **Clinical bronchiolitis obliterans in workers at a microwave-popcorn plant.** *N Engl J Med* 2002, **347:**330-338.
54. Farsalinos KE, Gillman G: **Carbonyl Emissions in E-cigarette Aerosol: A Systematic Review and Methodological Considerations.** *Front Physiol* 2017, **8:**1119.
55. Serbina NV, Jia T, Hohl TM, Pamer EG: **Monocyte-mediated defense against microbial pathogens.** *Annu Rev Immunol* 2008, **26:**421-452.

Legends:

Figure 1.Acute ENDS exposure induces parenchymal change and mucus accumulation in βENaC mice

(A) Experimental schematic of whole body ENDS exposure in βENaC mice. (B) ENDS exposure cause emphysematous phenotypes changes in βENaC-Tg mice. Representative data of H&E-stained section of sham air (left) (n=4) and ENDS exposure (right) (n=4) mice. (C) Quantitative morphometric analysis of alveolar septae of the lungs. (D) Representative images of Periodic Acid-Schiff staining in lung sections of βENaC mice without and with ENDS exposure. All data presented at mean +/- SEM (student t-test, ** $p< 0.01$).

Figure 2. ENDS exposure causes macrophage infiltration and inflammation in the lungs

(A) Representative images of Diff-Quik staining of BAL from βENaC mice without and with ENDS exposure (n=3 per group). (B) Quantitative analysis of cell number of BAL from βENaC mice without and with ENDS exposure. (C) Representative blots of cytokine protein expression by Mouse XL Cytokine Array in BAL fluid of βENaC mice without and with ENDS exposure (n=3 per group). (D-G) Protein expression of inflammatory cytokines, * $p<0.05$; ** $p<0.01$; *** $p<0.0001$.

Figure 3. ENDS exposure promotes small airway fibrosis. (A) Representative images of Pico-Sirius Red staining in lung sections from βENaC mice without and with ENDS exposure (n=3 per group). (B) Quantitative analysis of Sirius Red staining from βENaC mice with and without ENDS exposure (n=3 per group). (C) Representative images of Masson's Trichrome staining in lung sections from βENaC mice without and with ENDS exposure (n=3 per group). and (D) Quantitative analysis of Trichrome staining from βENaC mice with and without ENDS exposure (n=3 per group). (E) Representative images of α-SMA immunohistochemistry staining in lung sections from βENaC mice without and with ENDS exposure. (F) Quantitative analysis of α-SMA staining from βENaC mice without and with ENDS exposure (n=3 per group). * $p<0.05$; ** $p<0.01$; *** $p<0.0001$.

Figure 4. ENDS exposure causes lung vascular injury by inducing lung endothelial cell apoptosis

(A) Representative images of H&E and immunochemical staining of TUNEL (TdT-mediated dUTP nick end labeling, blue; counterstained by Red Counterstain C, red) in lung sections from βENaC mice. Green arrowheads indicate TUNEL positive cells. (B) Quantitative analysis of TUNEL staining from βENaC mice without and with ENDS exposure (n=3 per group). (C) Representative images of vWF (von Willebrand Factor) immunohistochemical staining of lung tissue from βENaC mice without and with ENDS exposure. (D) Quantitative analysis of vWF staining from βENaC mice without and with ENDS exposure (n=3 per group). The ratio of vWF positive vessels verses the field view. (F) Validation of apoptosis by Annexin V/PI analysis in human aortic endothelial cells (HAEC). HAEC were treated with ENDS w/o nicotine (bottom left) and ENDS with nicotine (bottom right) for 24h or 1 mM H_2O_2 (top right) for 12 hours as positive control and then processed

for Annexin V/PI apoptosis analysis by flow cytometry. (E) Quantification of Annexin V/PI assay. The cell viabilities were quantified as the Annexin V/ PI double-negative cell percentages of total acquired cells. Columns and error bars represent means ± SD, n=4 * $p<0.05$; ** $p<0.01$; *** $p<0.0001$.

Figure 5. ENDS exposure causes apoptosis in lung epithelial cells
(A) Representative images of H&E and immunochemical staining of TUNEL (TdT-mediated dUTP nick end labeling, blue; counterstained by Red Counterstain C, red) in lung sections from βENaC mice. Green arrowheads indicate TUNEL positive cells. (B) Quantitative analysis of TUNEL staining from βENaC mice without and with ENDS exposure (n=3 per group). (C) Validation of apoptosis by Annexin V/PI analysis in human lung epithelial cells (16HBE). The 16HBE cells were treated with, ENDS w/o nicotine and ENDS with nicotine for 24h or 1 mM H_2O_2 for 12 hours as positive control and then processed for Annexin V/PI apoptosis analysis by flow cytometry. (D) Quantification of Annexin V/PI assay. The cell viabilities were quantified as the Annexin V/ PI double-negative cell percentages of total acquired cells. Columns and error bars represent means ± SD, n=4 * $p<0.05$; ** $p<0.01$; *** $p<0.0001$.

Figure 6. Potential molecular mechanism of ENDS on inflammation, fibrosis, and apoptosis
The exposure of ENDS causes inflammation, fibrosis, and apoptosis of endothelial and epithelial in the lung. The acute inflammation leads to the production of IL-10 and IL-13, infiltration of macrophages, and mucus accumulation. Both cytokines are involved in the infiltration of immune cells and contribute to the inflammatory process. The elevation of macrophages in the lung was associated with fibrosis, collagen deposition, and myofibroblast differentiation. The acute ENDS exposure also stimulates the apoptosis in the endothelial and epithelial cells, which contribute to the destruction and degradation of lung alveoli.

Figures

Figure 1

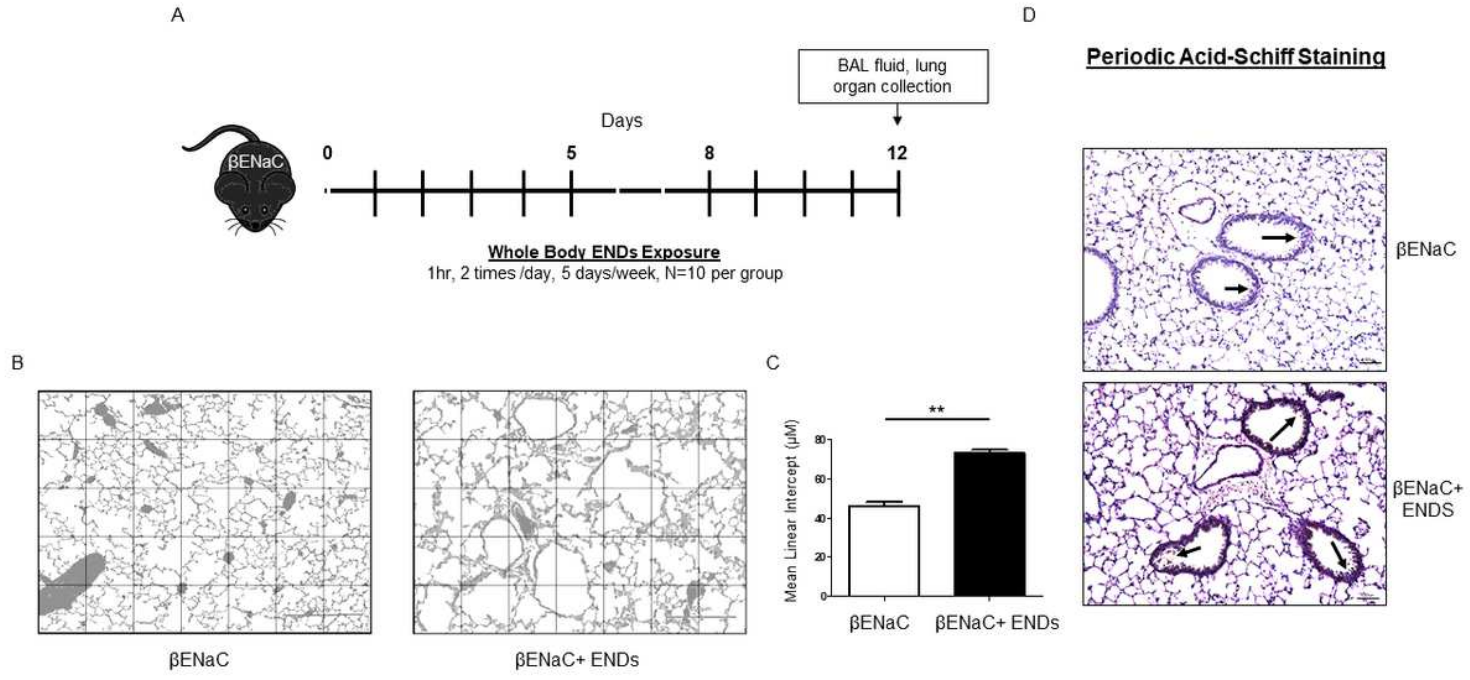

Figure 1

Acute ENDS exposure induces parenchymal change and mucus accumulation in βENaC mice (A) Experimental schematic of whole body ENDS exposure in βENaC mice. (B) ENDS exposure cause emphysematous phenotypes changes in βENaC-Tg mice. Representative data of H&E-stained section of sham air (left) (n=4) and ENDS exposure (right) (n=4) mice. (C) Quantitative morphometric analysis of alveolar septae of the lungs. (D) Representative images of Periodic Acid-Schiff staining in lung sections of βENaC mice without and with ENDS exposure. All data presented at mean +/- SEM (student t-test, ** p< 0.01).

Figure 1

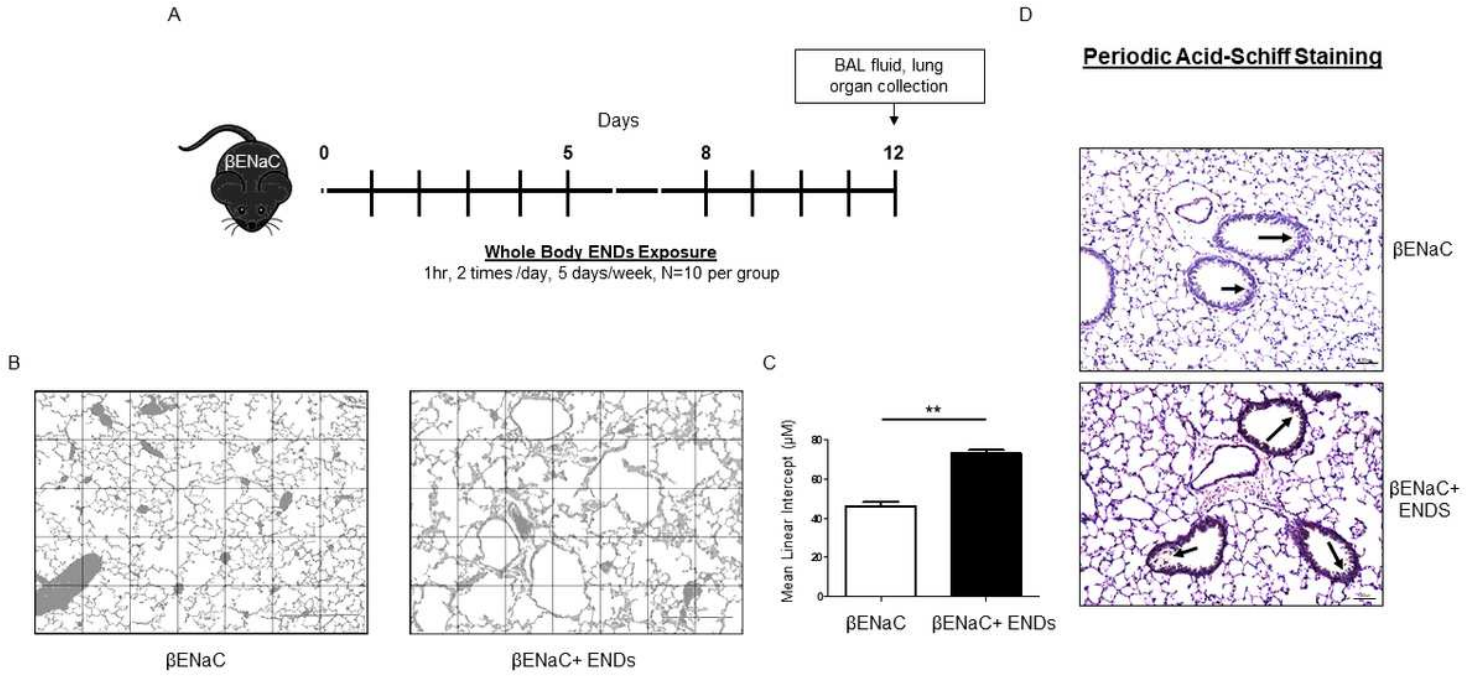

Figure 1

Acute ENDS exposure induces parenchymal change and mucus accumulation in βENaC mice (A) Experimental schematic of whole body ENDS exposure in βENaC mice. (B) ENDS exposure cause emphysematous phenotypes changes in βENaC-Tg mice. Representative data of H&E-stained section of sham air (left) (n=4) and ENDS exposure (right) (n=4) mice. (C) Quantitative morphometric analysis of alveolar septae of the lungs. (D) Representative images of Periodic Acid-Schiff staining in lung sections of βENaC mice without and with ENDS exposure. All data presented at mean +/- SEM (student t-test, ** p< 0.01).

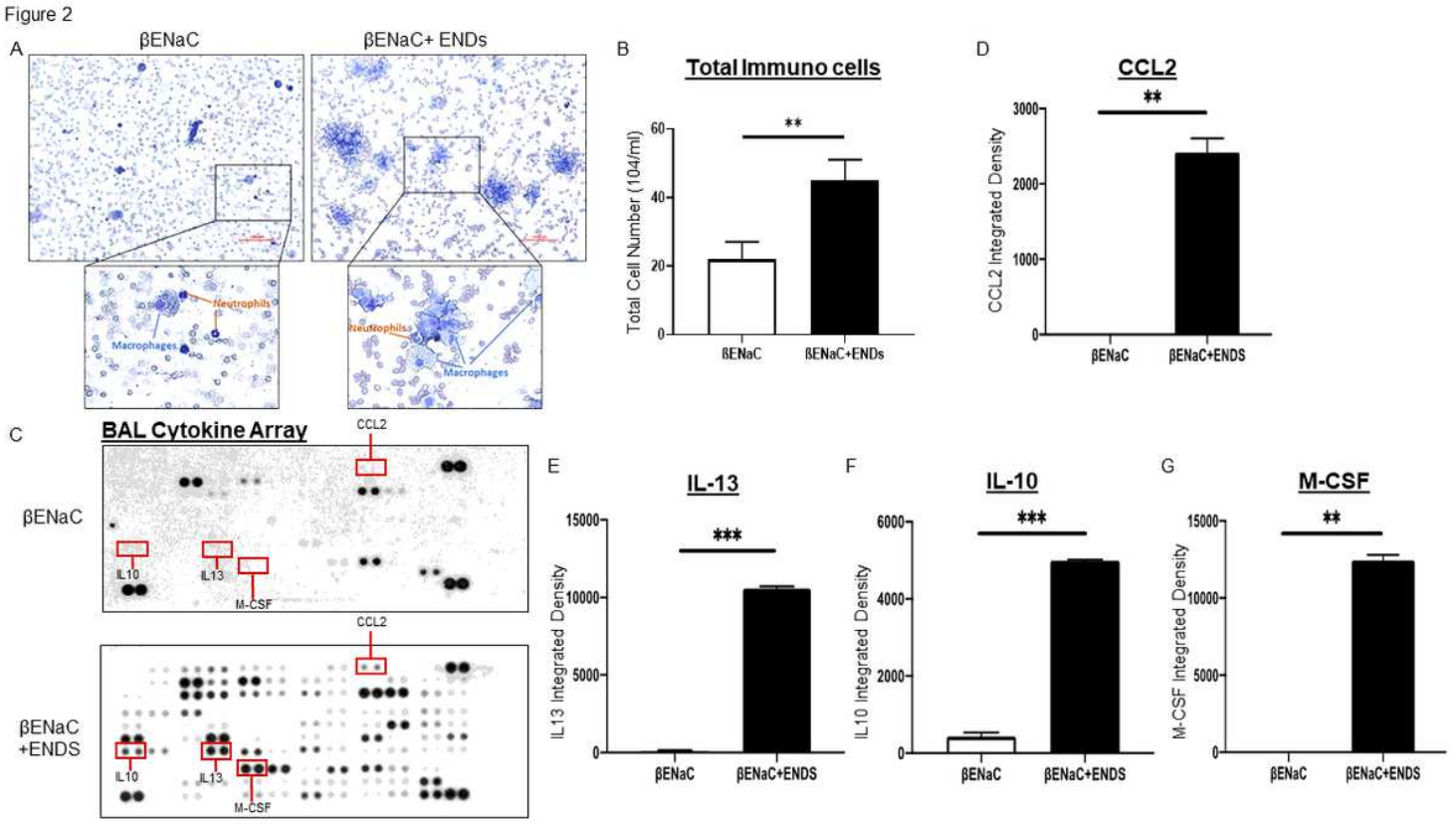

Figure 2

ENDS exposure causes macrophage infiltration and inflammation in the lungs (A) Representative images of Diff-Quik staining of BAL from βENaC mice without and with ENDS exposure (n=3 per group). (B) Quantitative analysis of cell number of BAL from βENaC mice without and with ENDS exposure. (C) Representative blots of cytokine protein expression by Mouse XL Cytokine Array in BAL fluid of βENaC mice without and with ENDS exposure (n=3 per group). (D-G) Protein expression of inflammatory cytokines, * $p<0.05$; ** $p<0.01$; *** $p<0.0001$.

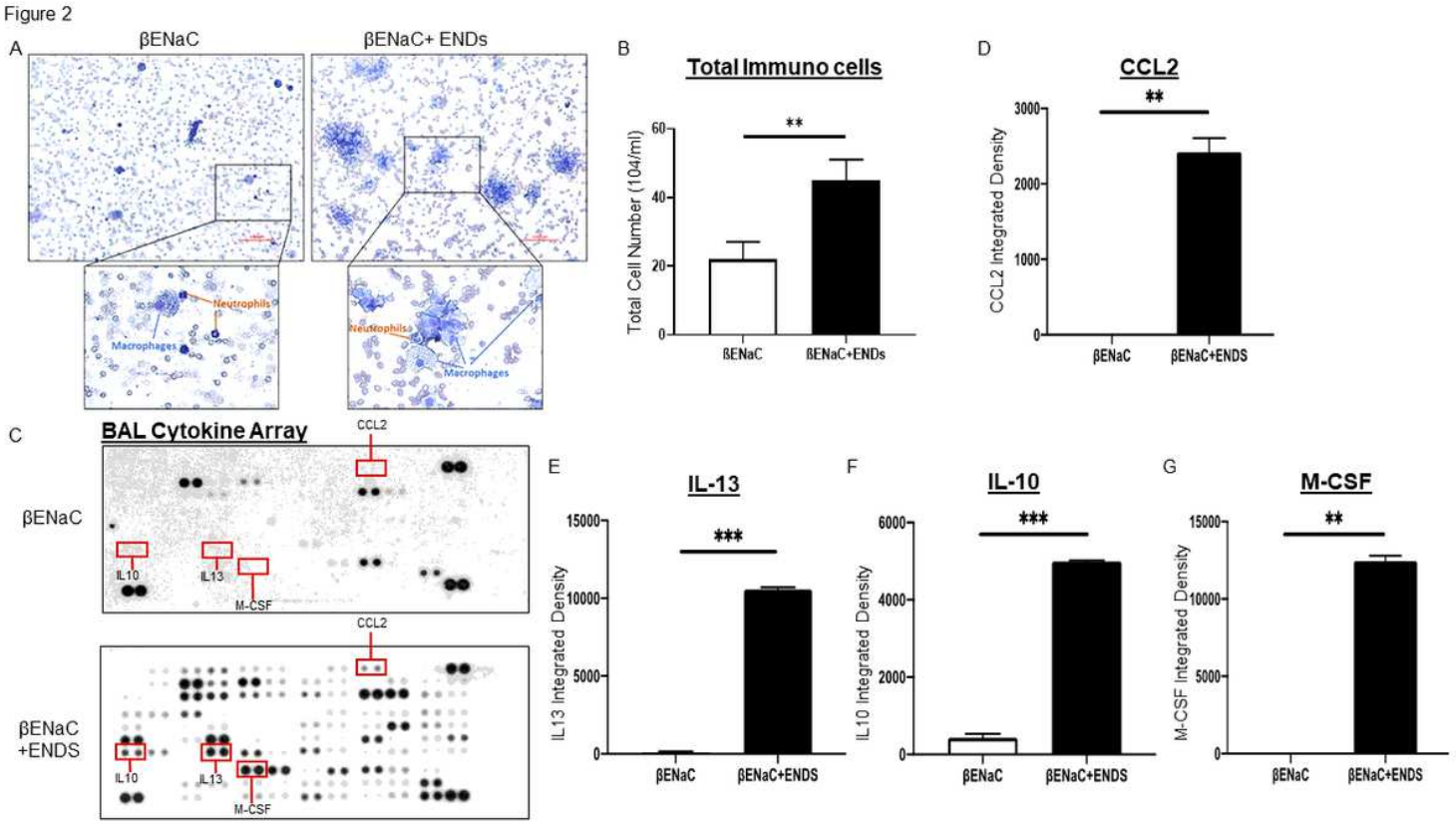

Figure 2

ENDS exposure causes macrophage infiltration and inflammation in the lungs (A) Representative images of Diff-Quik staining of BAL from βENaC mice without and with ENDS exposure (n=3 per group). (B) Quantitative analysis of cell number of BAL from βENaC mice without and with ENDS exposure. (C) Representative blots of cytokine protein expression by Mouse XL Cytokine Array in BAL fluid of βENaC mice without and with ENDS exposure (n=3 per group). (D-G) Protein expression of inflammatory cytokines, * $p<0.05$; ** $p<0.01$; *** $p<0.0001$.

Figure 3

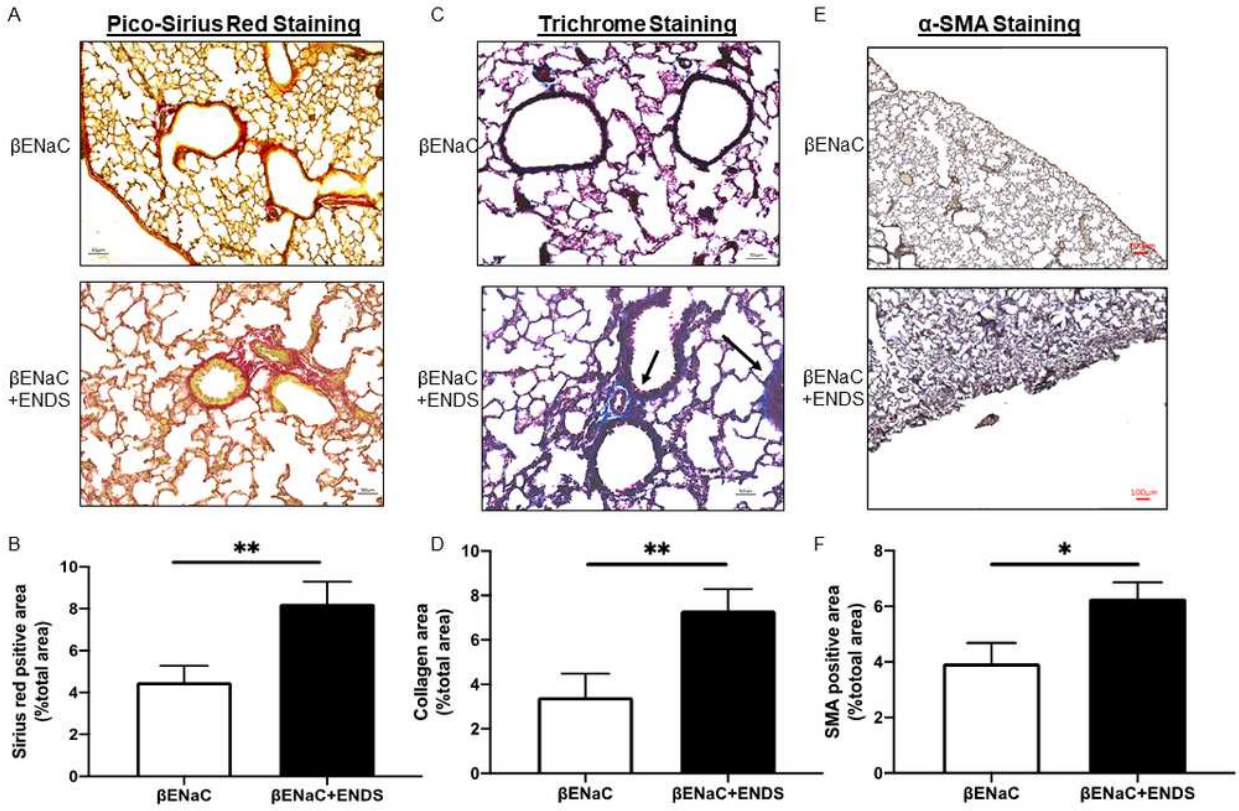

Figure 3

ENDS exposure promotes small airway fibrosis. (A) Representative images of Pico-Sirius Red staining in lung sections from βENaC mice without and with ENDS exposure (n=3 per group). (B) Quantitative analysis of Sirius Red staining from βENaC mice with and without ENDS exposure (n=3 per group). (C) Representative images of Masson's Trichrome staining in lung sections from βENaC mice without and with ENDS exposure (n=3 per group). and (D) Quantitative analysis of Trichrome staining from βENaC mice with and without ENDS exposure (n=3 per group). (E) Representative images of α-SMA immunohistochemistry staining in lung sections from βENaC mice without and with ENDS exposure. (F) Quantitative analysis of α-SMA staining from βENaC mice without and with ENDS exposure (n=3 per group). * $p<0.05$; **$p<0.01$; ***$p<0.0001$.

Figure 3

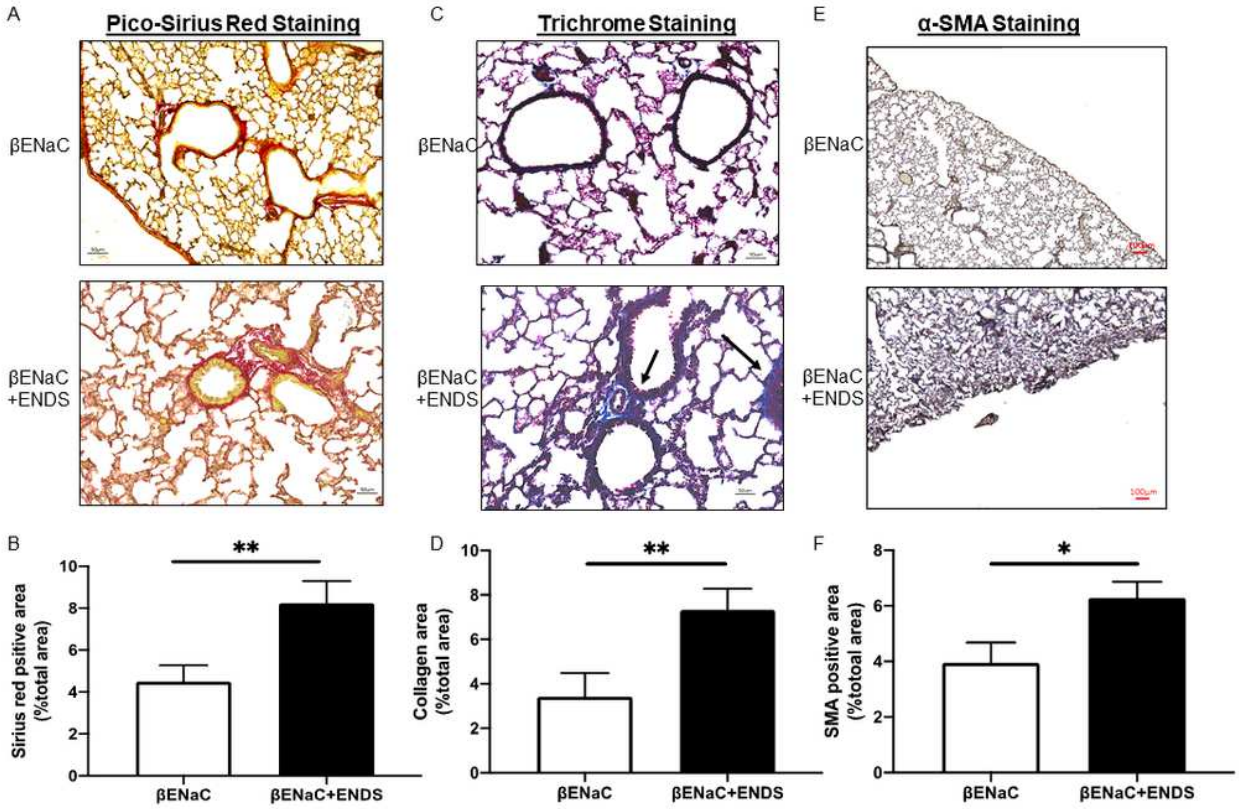

Figure 3

ENDS exposure promotes small airway fibrosis. (A) Representative images of Pico-Sirius Red staining in lung sections from βENaC mice without and with ENDS exposure (n=3 per group). (B) Quantitative analysis of Sirius Red staining from βENaC mice with and without ENDS exposure (n=3 per group). (C) Representative images of Masson's Trichrome staining in lung sections from βENaC mice without and with ENDS exposure (n=3 per group). and (D) Quantitative analysis of Trichrome staining from βENaC mice with and without ENDS exposure (n=3 per group). (E) Representative images of α-SMA immunohistochemistry staining in lung sections from βENaC mice without and with ENDS exposure. (F) Quantitative analysis of α-SMA staining from βENaC mice without and with ENDS exposure (n=3 per group). * $p<0.05$; **$p<0.01$; ***$p<0.0001$.

Figure 4

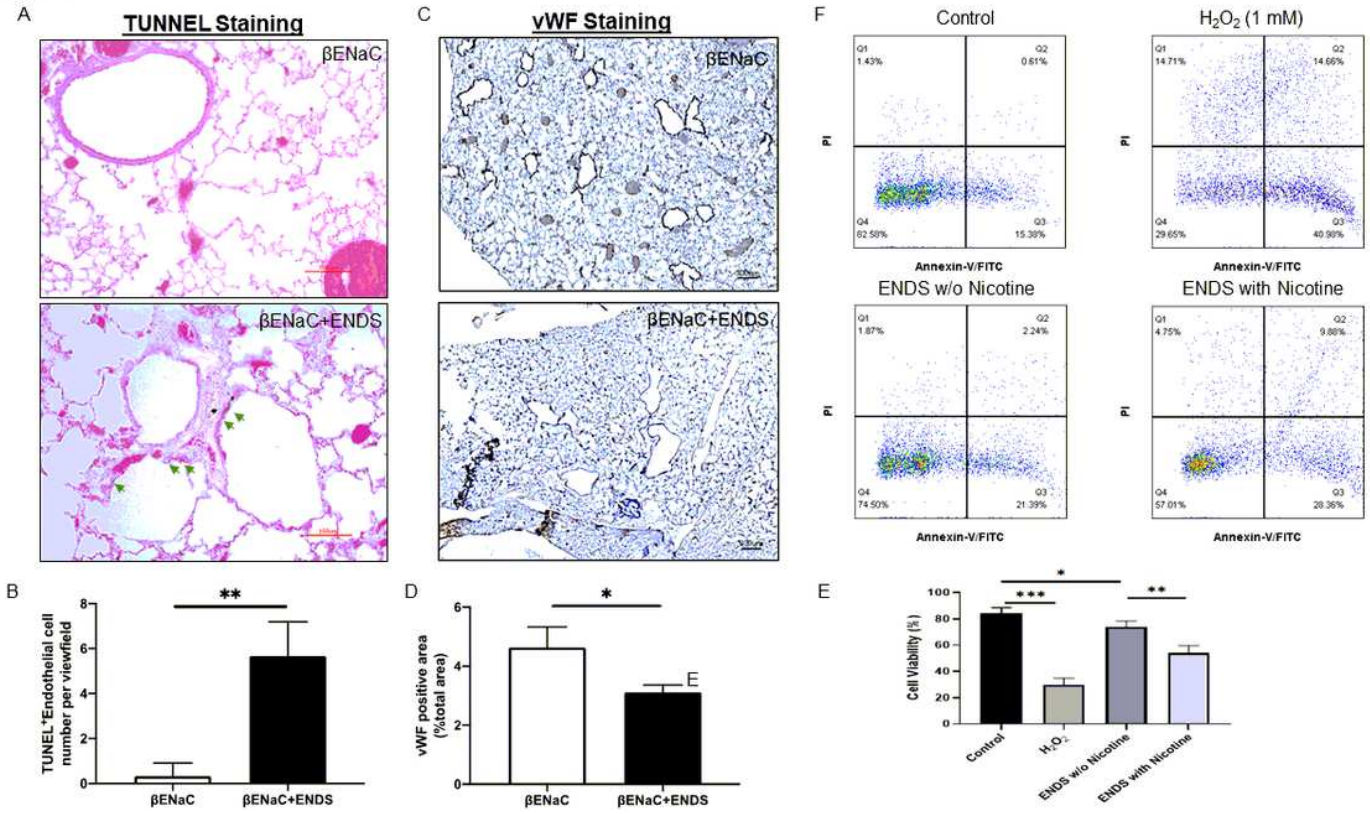

Figure 4

ENDS exposure causes lung vascular injury by inducing lung endothelial cell apoptosis (A) Representative images of H&E and immunochemical staining of TUNEL (TdT-mediated dUTP nick end labeling, blue; counterstained by Red Counterstain C, red) in lung sections from βENaC mice. Green arrowheads indicate TUNEL positive cells. (B) Quantitative analysis of TUNEL staining from βENaC mice without and with ENDS exposure (n=3 per group). (C) Representative images of vWF (von Willebrand Factor) immunohistochemical staining of lung tissue from βENaC mice without and with ENDS exposure. (D) Quantitative analysis of vWF staining from βENaC mice without and with ENDS exposure (n=3 per group). The ratio of vWF positive vessels verses the field view. (F) Validation of apoptosis by Annexin V/PI analysis in human aortic endothelial cells (HAEC). HAEC were treated with ENDS w/o nicotine (bottom left) and ENDS with nicotine (bottom right) for 24h or 1 mM H2O2 (top right) for 12 hours as positive control and then processed for Annexin V/PI apoptosis analysis by flow cytometry. (E) Quantification of Annexin V/PI assay. The cell viabilities were quantified as the Annexin V/ PI double-negative cell percentages of total acquired cells. Columns and error bars represent means ± SD, n=4 * p<0.05; **p<0.01; ***p<0.0001.

Figure 4

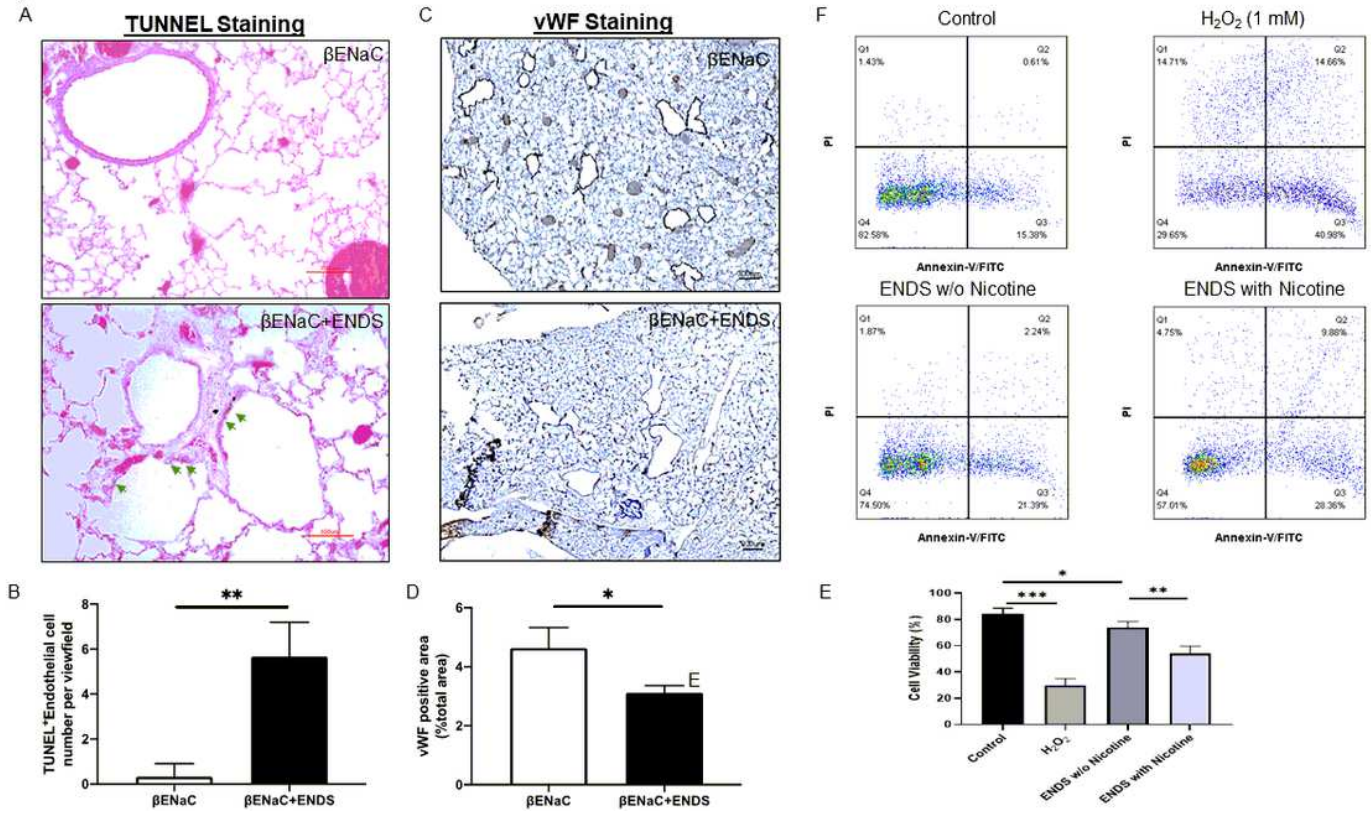

Figure 4

ENDS exposure causes lung vascular injury by inducing lung endothelial cell apoptosis (A) Representative images of H&E and immunochemical staining of TUNEL (TdT-mediated dUTP nick end labeling, blue; counterstained by Red Counterstain C, red) in lung sections from βENaC mice. Green arrowheads indicate TUNEL positive cells. (B) Quantitative analysis of TUNEL staining from βENaC mice without and with ENDS exposure (n=3 per group). (C) Representative images of vWF (von Willebrand Factor) immunohistochemical staining of lung tissue from βENaC mice without and with ENDS exposure. (D) Quantitative analysis of vWF staining from βENaC mice without and with ENDS exposure (n=3 per group). The ratio of vWF positive vessels verses the field view. (F) Validation of apoptosis by Annexin V/PI analysis in human aortic endothelial cells (HAEC). HAEC were treated with ENDS w/o nicotine (bottom left) and ENDS with nicotine (bottom right) for 24h or 1 mM H2O2 (top right) for 12 hours as positive control and then processed for Annexin V/PI apoptosis analysis by flow cytometry. (E) Quantification of Annexin V/PI assay. The cell viabilities were quantified as the Annexin V/ PI double-negative cell percentages of total acquired cells. Columns and error bars represent means ± SD, n=4 * p<0.05; **p<0.01; ***p<0.0001.

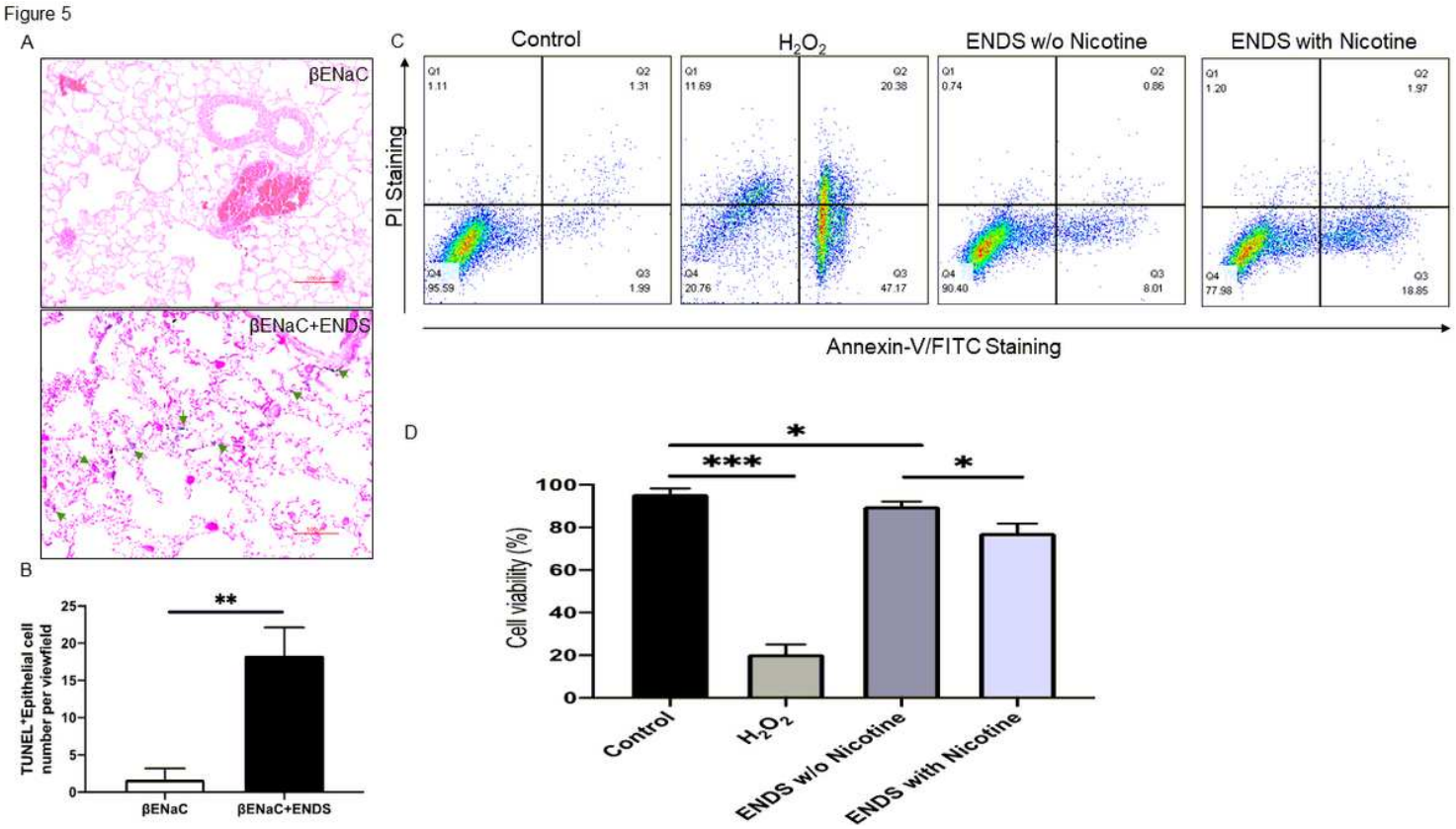

Figure 5

ENDS exposure causes apoptosis in lung epithelial cells (A) Representative images of H&E and immunochemical staining of TUNEL (TdT-mediated dUTP nick end labeling, blue; counterstained by Red Counterstain C, red) in lung sections from βENaC mice. Green arrowheads indicate TUNEL positive cells. (B) Quantitative analysis of TUNEL staining from βENaC mice without and with ENDS exposure (n=3 per group). (C) Validation of apoptosis by Annexin V/PI analysis in human lung epithelial cells (16HBE). The 16HBE cells were treated with, ENDS w/o nicotine and ENDS with nicotine for 24h or 1 mM H2O2 for 12 hours as positive control and then processed for Annexin V/PI apoptosis analysis by flow cytometry. (D) Quantification of Annexin V/PI assay. The cell viabilities were quantified as the Annexin V/ PI double-negative cell percentages of total acquired cells. Columns and error bars represent means ± SD, n=4 * p<0.05; **p<0.01; ***p<0.0001.

Figure 5

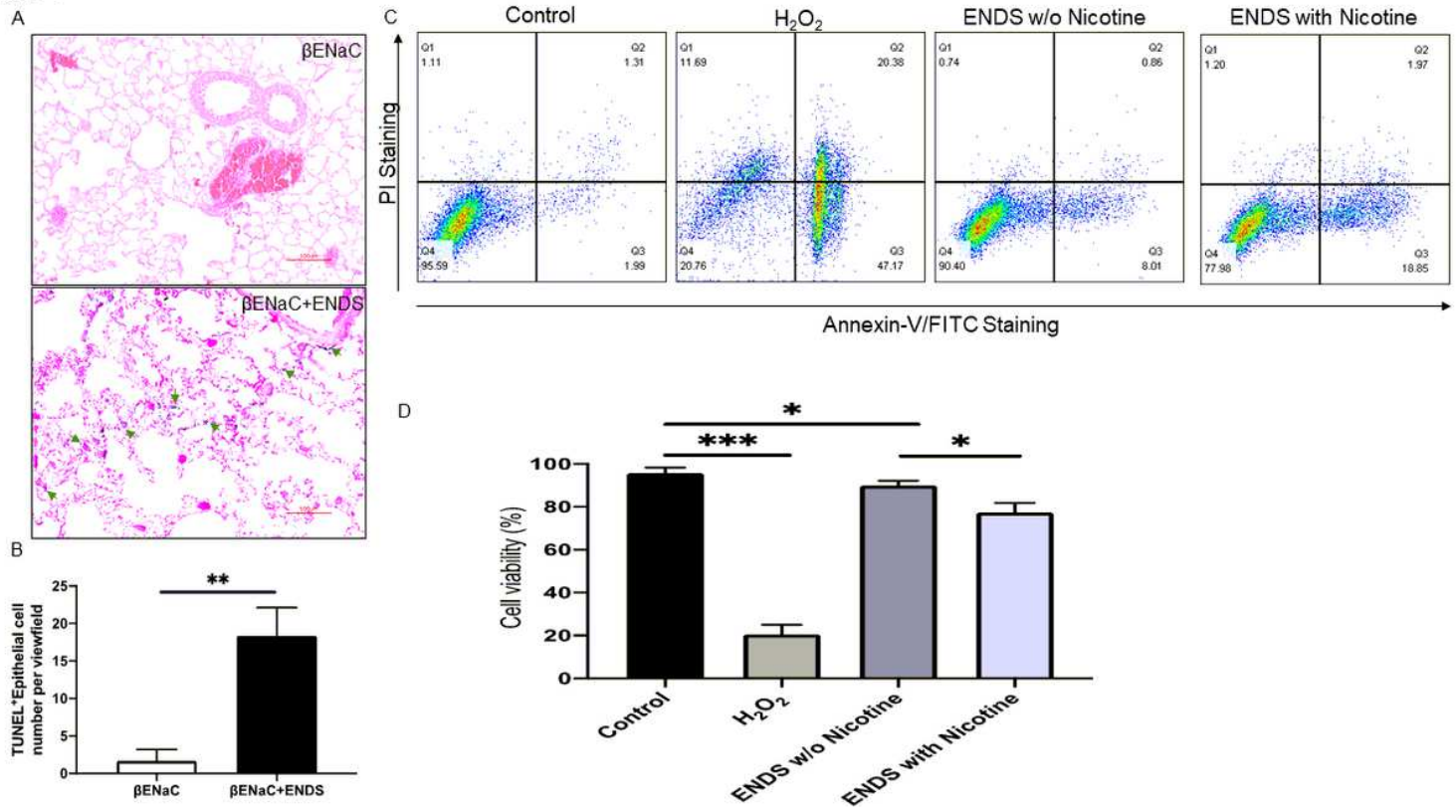

Figure 5

ENDS exposure causes apoptosis in lung epithelial cells (A) Representative images of H&E and immunochemical staining of TUNEL (TdT-mediated dUTP nick end labeling, blue; counterstained by Red Counterstain C, red) in lung sections from βENaC mice. Green arrowheads indicate TUNEL positive cells. (B) Quantitative analysis of TUNEL staining from βENaC mice without and with ENDS exposure (n=3 per group). (C) Validation of apoptosis by Annexin V/PI analysis in human lung epithelial cells (16HBE). The 16HBE cells were treated with, ENDS w/o nicotine and ENDS with nicotine for 24h or 1 mM H2O2 for 12 hours as positive control and then processed for Annexin V/PI apoptosis analysis by flow cytometry. (D) Quantification of Annexin V/PI assay. The cell viabilities were quantified as the Annexin V/ PI double-negative cell percentages of total acquired cells. Columns and error bars represent means ± SD, n=4 * p<0.05; **p<0.01; ***p<0.0001.

Figure 6

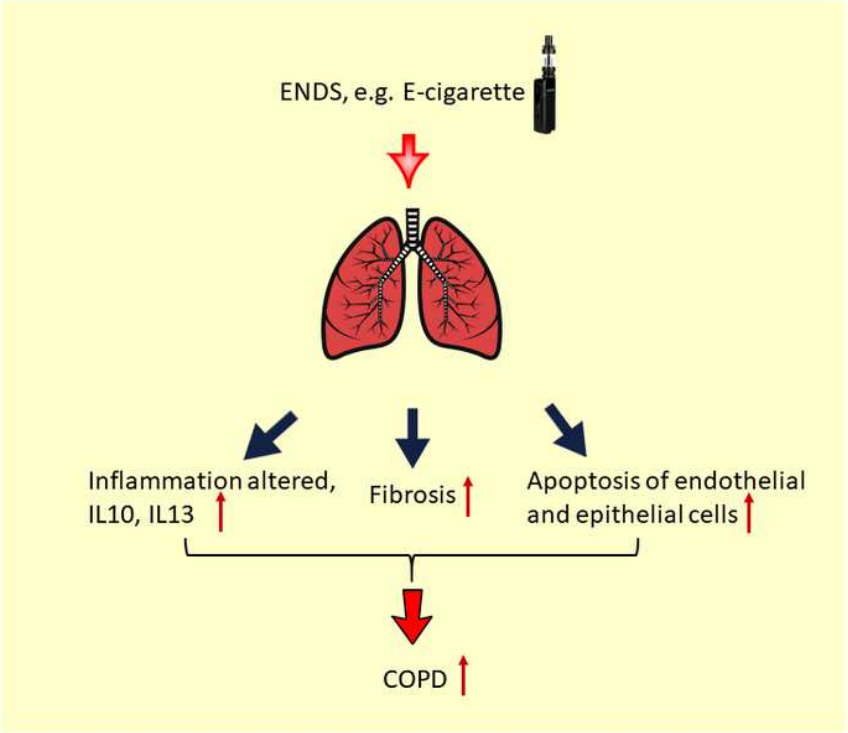

Figure 6

Potential molecular mechanism of ENDS on inflammation, fibrosis, and apoptosis The exposure of ENDS causes inflammation, fibrosis, and apoptosis of endothelial and epithelial in the lung. The acute inflammation leads to the production of IL-10 and IL-13, infiltration of macrophages, and mucus accumulation. Both cytokines are involved in the infiltration of immune cells and contribute to the inflammatory process. The elevation of macrophages in the lung was associated with fibrosis, collagen deposition, and myofibroblast differentiation. The acute ENDS exposure also stimulates the apoptosis in the endothelial and epithelial cells, which contribute to the destruction and degradation of lung alveoli.

Figure 6

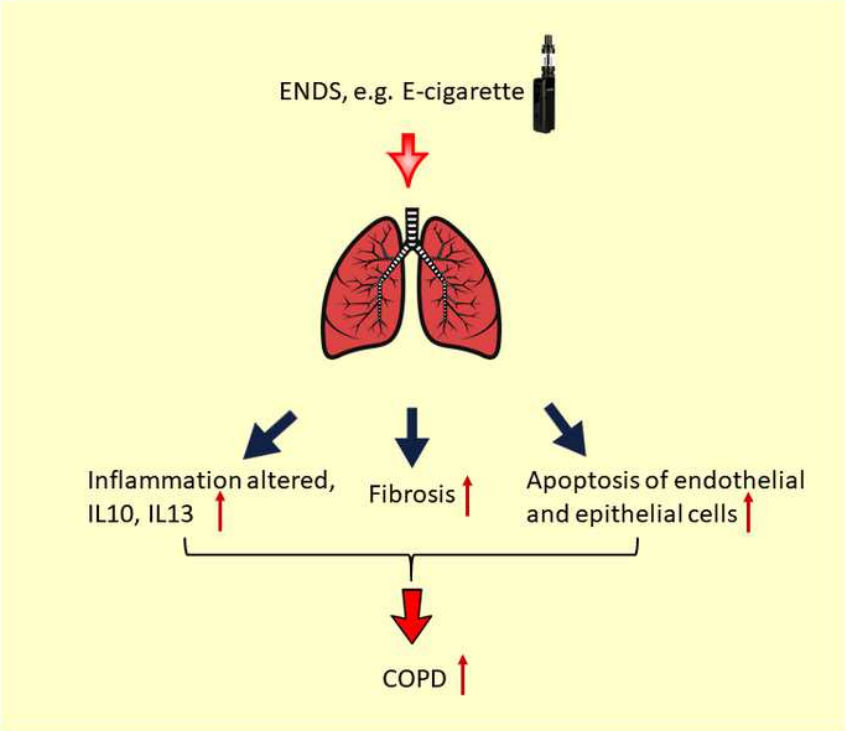

Figure 6

Potential molecular mechanism of ENDS on inflammation, fibrosis, and apoptosis The exposure of ENDS causes inflammation, fibrosis, and apoptosis of endothelial and epithelial in the lung. The acute inflammation leads to the production of IL-10 and IL-13, infiltration of macrophages, and mucus accumulation. Both cytokines are involved in the infiltration of immune cells and contribute to the inflammatory process. The elevation of macrophages in the lung was associated with fibrosis, collagen deposition, and myofibroblast differentiation. The acute ENDS exposure also stimulates the apoptosis in the endothelial and epithelial cells, which contribute to the destruction and degradation of lung alveoli.